Electrochimica Acta 54 (2009) 5500–5508

Contents lists available at ScienceDirect

Electrochimica Acta

journal homepage: www.elsevier.com/locate/electacta

Synthesis, characterization and electrochemical properties of a novel triphosphate $LiFe_2P_3O_{10}$

M. Kopec[a], C.V. Ramana[b], X. Zhang[c], A. Mauger[c,*], F. Gendron[a], J.-F. Morhange[a], K. Zaghib[d], C.M. Julien[a]

[a] Institut des Nano-Sciences de Paris (INSP), Université Pierre et Marie Curie, Campus Boucicaut, 140 rue de Lourmel, 75015 Paris, France
[b] Nanoscience and Surface Chemistry Laboratory, Department of Geological Sciences, University of Michigan, Ann Arbor, MI 48109, USA
[c] Institut de Minéralogie et de Physique des Milieux Condensés, Campus Boucicaut, 140 rue de Lourmel, 75015 Paris, France
[d] Institut de Recherche d'Hydro-Québec (IREQ), 1800 boul. Lionel-Boulet, Varennes, Québec, J3X 1S1, Canada

ARTICLE INFO

Article history:
Received 24 February 2009
Received in revised form 17 April 2009
Accepted 18 April 2009
Available online 3 May 2009

Keywords:
Lithium batteries
Lithium iron triphosphate
Structure
Vibrational spectroscopy
Magnetic susceptibility
Voltammetry

ABSTRACT

A novel lithium iron phosphate has been synthesized by a solution route at moderate temperature. The structure was determined from powder by XRD, HRTEM and SAED experiments. $LiFe_2P_3O_{10}$ tripolyphosphate crystallizes in the monoclinic system, space group $P2_1/m$, with lattice constants $a = 4.597(7)$ Å, $b = 8.566(4)$ Å, $c = 9.051(4)$ Å, $\beta = 97.47^\circ$ and $Z = 2$. Internal and external vibrational modes (Raman and FTIR) show that the dominant spectral features come from the $(P_3O_{10})^{5-}$ oxo-anions displaying internal and external modes along with the P–O–P bridging modes. Magnetic measurements are consistent with the high-spin configuration of Fe^{2+} cation with an effective magnetic moment 5.51 μ_B. A weak antiferromagnetic ordering is observed below the Néel temperature at $T_N = 19$ K. Electron paramagnetic resonance spectroscopy confirms this electronic configuration and provides evidence of the presence of a carbonaceous layer onto the particle surface. Electrochemical measurements were carried out in lithium cells with $LiPF_6$–EC–DEC electrolyte at 25 °C. The material delivered a capacity 70 mAh/g in the voltage range 2.7–3.9 V, close to the theoretical value (72 mAh/g). The resulting cyclic voltammogram indicates a stable structure with a good reversibility with the redox peaks at 3.26 and 3.13 V vs. Li^0/Li^+.

1. Introduction

Lithium iron phosphates composed by the assembly of $[P_nO_{3n+1}]^{(n+2)-}$ polyanions (with $n = 1$ and 2) have received much attention as high-potential positive electrode materials for rechargeable Li-ion batteries [1–3]. Typical materials include either Fe(II) cations such as the olivine-like structure $LiFePO_4$, or Fe(III) cations such as the Nasicon-like compound $Li_3Fe_2(PO_4)_3$ and the diphosphate $LiFeP_2O_7$ [4,5].

The main advantages of materials with polyanions such as $(PO_4)^{3-}$, $(P_2O_7)^{4-}$, or $(P_3O_{10})^{5-}$ is their thermal stability that improves safety at high temperatures. Also they contain non-toxic elements and show remarkable features in rechargeable lithium-ion batteries [3]. For use as electrode, the main problems that need to be solved are major structural anomalies, such as anisotropic deformation, significant loss of long-range order, local phase segregation and clustering impurities [6]. The search for iron phosphate materials having Fe^{2+} ions has attracted our interest towards framework built with $(P_3O_{10})^{5-}$ oxo-anions. The strong inductive effect of the assembly of interconnected $(PO_4)^{3-}$ polyanions is expected to moderate the Fe^{2+}/Fe^{3+} redox couple to generate a high operating potential.

The structure of $AB_2P_3O_{10}$ compounds where A is an alkali ion and B a divalent cation is a three-dimensional lattice formed by the connection of BO_6 ocatahedra and P_3O_{10} groups formed by three shared-corner PO_4 tetrahedral units. This assembly contains tunnels running parallel to the b-axis in which are located the A^+ cations. Fig. 1 shows a schematic representation of the $LiM_2P_3P_{10}$ framework where M is a transition metal. Few works concerning the $AB_2P_3O_{10}$ phases have been reported in the literature. Only $RbBe_2P_3O_{10}$ and $LiCo_2P_3O_{10}$ are known as anhydrous phases [7–9], while several hydrated compounds such as $KCu_2P_3O_{10}{\cdot}5H_2O$, $LiZn_2P_3O_{10}{\cdot}8H_2O$, and $NaZn_2P_3O_{10}{\cdot}9H_2O$ have been investigated [10–13].

The aim of this work is the wet-chemical synthesis and the characterization of lithium di-iron triphosphate $LiFe_2P_3O_{10}$, to understand the structural features and the morphology that are of crucial importance in the design of new electrode materials for lithium battery technology. In this context, crystal chemistry has been studied using X-ray diffractometry (XRD) and analytical transmission electron microscopy including high-resolution transmission electron microscopy (HRTEM) and selected area electron diffraction (SAED). Physical characterizations include Fourier transform infrared (FTIR), Raman scattering (RS) spectroscopy, SQUID

* Corresponding author. Tel.: +33 14427 4439.
E-mail address: alain.mauger@impmc.jussieu.fr (A. Mauger).

0013-4686/$ – see front matter © 2009 Elsevier Ltd. All rights reserved.
doi:10.1016/j.electacta.2009.04.050

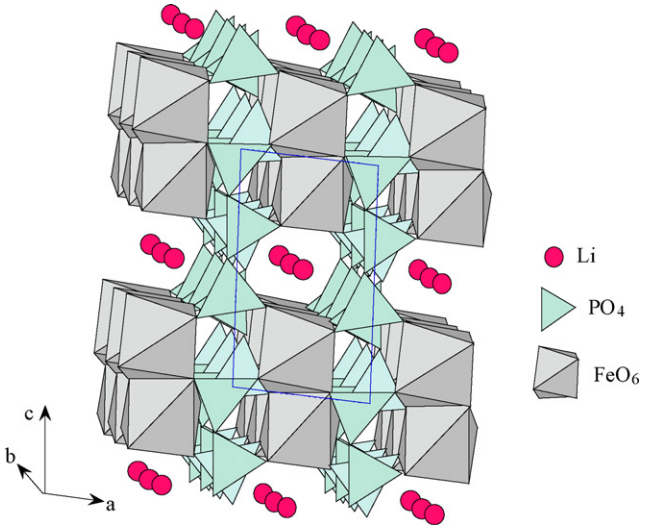

Fig. 1. Schematic representation of the polyhedral structure of $LiFe_2P_3O_{10}$. The triphosphate network is built by FeO_6 octahedra and P_3O_{10} groups forming tunnels within which the Li^+ ions are located.

magnetometry and electron spin resonance (ESR) spectroscopy. The lithium insertion-extraction ability of $LiFe_2P_3O_{10}$ is investigated by slow-scan cyclic voltammetry in $Li/LiPF_6$ – ethylene carbonate–diethylene carbonate (EC–DEC)/$LiFe_2P_3O_{10}$ cell.

2. Experimental

2.1. Sample preparation

Samples of lithium iron triphosphate, $LiFe_2P_3O_{10}$ were synthesized by a solution route at moderate temperature using Fe^{2+} precursor compound, typically iron(II) acetate. In this wet-chemical method, we used lithium acetate dihydrate $LiOOCCH_3{\cdot}2H_2O$, iron acetate monohydrate $Fe(OOCCH_3)_2{\cdot}H_2O$ and phosphoric(V) acid H_3PO_4 (Fluka purum grade) as starting materials. Raw materials were mixed in a molar ratio of Li:Fe:P = 1.05:1:1 in N,N-dimethylformamide with careful stirring during 24 h. Excess of lithium is needed to prevent loss of stoichiometry in the final product. The solvent was slowly evaporated at 120 °C in air. After a careful grinding the solid dry residue was pre-heated at 350 °C for 2 h for the formation of the phosphate precursor. Successive grinding operations were performed before the final heated treatment at 600 °C for 24 h. The calcination procedures were carried out in a flow of Ar/H_2 gas (85:15) to prevent any oxidation of iron into Fe^{3+} ions. A grey fine powder was then obtained and characterized by various analytical techniques to check the purity of the resulting phase.

A carbon coating is obtained by sintering this samples with a carbon precursor (lactose) at 700 °C during 12 h. The experiments reported in this work have been made on carbon-coated samples, since they are of better quality. Data for electrochemical properties are reported for both samples for comparison, confirming the better performance of carbon-coated samples for the same reasons as in the case of $LiFePO_4$ [2,14,16].

2.2. Instruments

The X-ray diffractograms (XRD) has been recorded on a Philips X'Pert PRO MRD (PW3050) diffractometer equipped with a Cu anticathode (CuK_α radiation $\lambda = 1.54056$ Å) at room temperature. The measurements have been recorded under Bragg-Brentano geometry at 2θ with step 0.05° in the range 10–80°. SEM observations were realized by a high resolution electron microscope Hitachi (S-4700). The powders were sprinkled on a adhesive carbon ribbon to obtain a thin film of particles. TEM analysis was performed using a Jeol TEM2010F at a 200 kV acceleration voltage. Phase and structure of the material were monitored using selected area electron diffraction (SAED). Specimen for TEM analysis was prepared by dispersing the $LiFe_2P_3O_{10}$ sample on 3 mm Cu grid with a hole size of 1 mm × 2 mm. High resolution transmission electron microscopy (HRTEM) image processing including the fast Fourier transformation (FFT) was carried out by Gatan Digital Micrograph 3.4.

Fourier transform infrared (FTIR) absorption spectra were recorded using a Bruker IFS 113 vacuum interferometer. In the far infrared region (400–100 cm^{-1}), the vacuum bench apparatus was equipped with a 3.5 μm-thick Mylar beam splitter, a globar source and a DTGS/PE far-infrared detector. Raman spectra were measured in the high-wavenumber region 800–1800 cm^{-1} using a Jobin-Yvon U1000 double pass spectrometer equipped with a cooled, low noise photomultiplier tube (ITT FW130). The incident light used for the experiments was the 515 nm Ar line of a laser source. The susceptibility and magnetization were measured using a superconducting quantum interference device (SQUID) magnetometer (Quantum Design MPMS). The data were recorded in both the zero-field cool (ZFC) and field cool (FC) mode with a magnetic field of $H = 10$ kOe. The derivative signals of the ESR absorption spectra have been recorded with the use of an X-band Varian spectrometer. The powder samples have been placed in an ESR Oxford Instruments continuous flow cryostat, allowing measurements in the whole temperature range between room temperature and 3.5 K. The cryostat itself was inserted in a TE 102 microwave cavity. The frequency of the microwave field was 9.25 GHz. The frequency of the ac-modulation magnetic field was 100 kHz, and the dc magnetic field varied in the range 0–20 kOe.

The electrochemical properties of the product were tested at 25 °C in cells with metallic lithium as negative electrode using Teflon laboratory-cell hardware and Mac-Pile system. The non-aqueous electrolyte was the DEC-EC mixture (1:1 in volume) containing 1.0 mol/dm^3 $LiPF_6$. Cyclic voltammograms were carried out in the potential range V vs. Li^0/Li^+ at slow scan rate 20 mV/h.

3. Results and discussion

3.1. Structure and morphology

Fig. 2 shows the XRD diagram of the $LiFe_2P_3O_{10}$ powders calcined at 600 °C in hydrogen-containing atmosphere. The X-ray diffraction data for the $LiFe_2P_3O_{10}$ phase are indexed on the monoclinic unit cell in space group $P2_1/m \equiv C_{2h}^2$. It is evidenced that XRD pattern is dominated by the intense (1 2 0) line recorded at $d = 3.11$ Å and six lines with moderate intensity located at $d = 5.345$, 3.358, 2.703 and 2.510 Å corresponding to the (1 0 1), (1 1 1), ($\bar{1}$02), ($\bar{1}$21), (1 1 2) and ($\bar{1}$03) indexes, respectively (Table 1). The lattice constants have been calculated to be $a = 4.597(7)$ Å, $b = 8.566(4)$ Å, $c = 9.051(4)$ Å, $\beta = 97.47°$ and the elementary cell volume is $V = 353.5$ Å^3 with $Z = 2$. These values are consistent with those reported for the isomorphic materials such as $LiCo_2P_3O_{10}$ and $LiNi_2P_3O_{10}$ [8].

The $(P_3O_{10})^{5-}$ groups are formed by the linear chain constituted of three shared corner $(PO_4)^{3-}$ units (Fig. 3). The main interest of the atomic arrangement in $LiFe_2P_3O_{10}$ is the new type of configuration for the $(P_3O_{10})^{5-}$ groups. The three phosphorus atoms and the two bonding oxygen atoms are located on the mirror plane of the internal symmetry of the oxo-anions with successive PO_3 moities displaying both staggered and eclipsed conformations [9]. Thus the average value of the P–O–P bridging angle is found to be around 134° which is a value close to that found for $Na_5P_3O_{10}$ [15]. The iron atoms display distorted octahedral coordination. In the FeO_6 chain,